

EXPERIMENTAL AND MODELING ANALYSES OF AI-BASED NANOCOMPOSITES MANUFACTURED VIA MOLTEN-METAL AND SOLIDIFICATION PROCESSING ASSISTED BY ULTRASONIC STIRRING TECHNOLOGY*

Shian Jia¹
Daojie Zhang²
Laurentiu Nastac³

Abstract

Ultrasonic Stirring Technology (UST) is used in this study to manufacture Al-based nano-composites. Ultrasonic cavitation plays an important role in refining the microstructure, dispersing the nanoparticles and breaking up clusters of nanoparticles. In this paper, 6061/A356 alloys and Al₂O₃/SiC nanoparticles are used as the matrix alloys and the reinforcements, respectively. The nanoparticles were inserted into the molten alloy and dispersed by ultrasonic cavitation and acoustic streaming. A previously developed multiphase Computational Fluid Dynamics (CFD) model was used to study the cavitation and the nanodispersion phenomena during ultrasonic processing of these alloys. A comparison between the mechanical properties of the as-cast 6061 and 356 alloys and nano-composites has been performed.

Keywords: Ultrasonic stirring; 6061 and 356 alloys and nanocomposites; SiC and Al₂O₃ nanoparticles; Evaluation of mechanical properties.

¹ M.S. in Materials Science and Engineering, Ph.D. Student, MTE Department, The University of Alabama, Tuscaloosa, USA.

² M.S. in Materials Science and Engineering, Ph.D. Student, MTE Department, The University of Alabama, Tuscaloosa, USA.

³ Ph.D. in Metallurgical and Materials Engineering, Professor of Metallurgical and Materials Engineering, MTE Department, The University of Alabama, Tuscaloosa, USA.

1 INTRODUCTION

Al-based nanocomposites can offer outstanding properties, including low density, high specific strength, high specific stiffness, excellent wear resistance and controllable expansion coefficient, which make them attractive for numerous applications in aerospace, automobile, and military industries field [1-11].

UST has been extensively used in purifying, degassing, and refinement of metallic melt [12-16], mainly because introducing the ultrasonic energy into a liquid will induce cavitation and acoustic streaming. Ultrasonic cavitation in liquids causes high speed liquid jets of up to about 300 m/s. Such jets press liquid at high pressure between the particles and separate them from each other [17]. Acoustic streaming is a steady motion of the fluid driven by the absorption of high amplitude acoustic oscillations. Ultrasonic stirring technology can also improve the wettability between the reinforced nanoparticles and the metal matrix, which will assist to distribute the nanoparticles more uniformly into the metal matrix [18-20].

Al₂O₃ and SiC are widely used as reinforcement particles due to their relatively good thermal and chemical stability. In this study, the effects of the ultrasonically dispersed Al₂O₃ and SiC nanoparticles on the microstructure and mechanical properties of A356 and 6061 nano-composites are shown.

2 EXPERIMENTAL TECHNIQUE

Aluminum alloy A356 and 6061 were selected as the metallic matrix. The nominal chemical composition of the alloys are shown in Table 1. The ceramic nanoparticles used in this study were β -SiC (spherical shape, average diameter of about 50 nm) and Al₂O₃ (spherical shape, average diameter of 20 nm).

Table 1. Nominal chemical composition of matrix alloys studied (in wt. %)

Matrix Alloy	Si	Fe	Cu	Mn	Mg	Zn	Ti	Balance
A356	6.5-7.5	0.20	0.20	0.10	0.25-0.45	0.10	0.20	Al
6061	0.4-0.8	0.70	0.15-0.4	0.15	0.8-1.2	0.25	0.15	Al

The ultrasonic processing system used in this study is illustrated in Figure 1. The main parameters of the ultrasonic equipment are: maximum power, $P = 2.4\text{kW}$ and frequency, $f = 18\text{ kHz}$. An induction furnace with a capacity of 2.7 kg was used to melt the alloys. After the alloy is melted, the Nb ultrasonic probe was inserted to about 50 mm beneath the melt surface to perform ultrasonic stirring at a power of 1.75 kW. 1 wt% nanoparticles (Al₂O₃ or SiC) were injected into the cavitation area (beneath the ultrasonic probe) during a 15 min time-frame. The molten pool was protected by Argon gas atmosphere. A thermocouple was used to monitor the melt temperature to control the superheat. A higher pouring temperature of 750°C was used to minimize the formation of metal-mold filling defects including cold-shuts. The metal mold was preheated to 400°C. The specimen was extracted from the metal mold after 30 min and tested on a tensile test machine. The dimensions of the specimen are 50.8 mm length and 12.7 mm diameter. The experiments were repeated several times for statistical interpretation of the results.

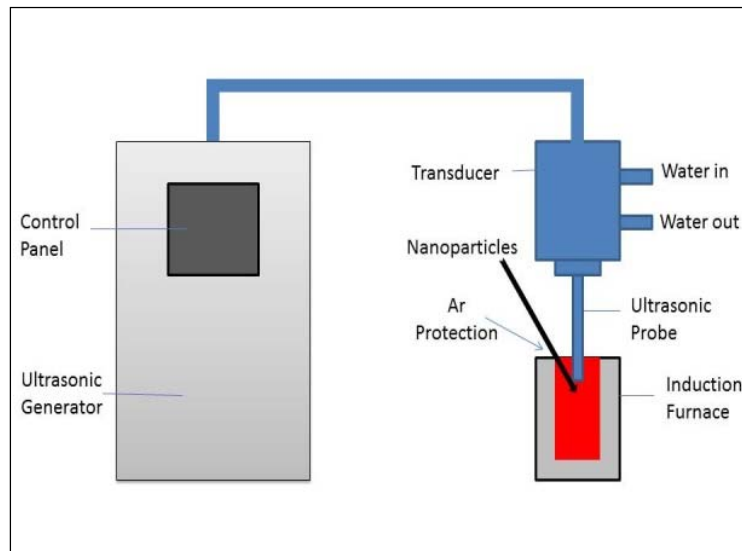


Figure 1. A schematic representation of the UST-induction furnace equipment.

3 MODELING TECHNIQUE

The geometry of the model is shown in Fig 2. The ultrasonic probe has a diameter of 40 mm. The liquid aluminum is 6061 and A356. The SiC and Al₂O₃ are treated as inert-particles. The mass flow rate of the nanoparticles is 0.014 kg/s. Thus, 1.0 wt.% of nanoparticles can be injected at about 20 mm above the bottom of the furnace for 1.0 sec.

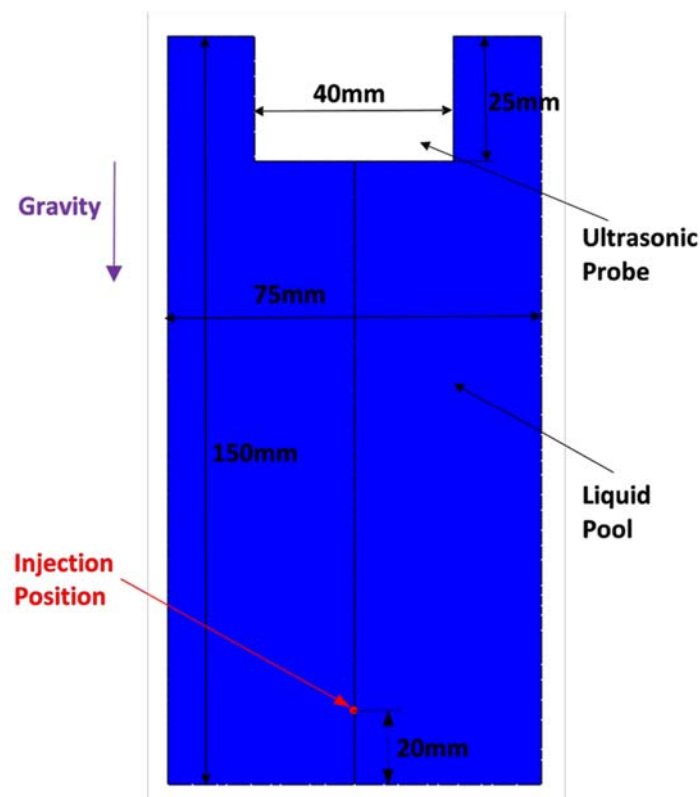


Figure 2. Geometry of model.

The multiphase CFD model is able to account for cavitation, turbulent fluid flow, heat transfer, solidification and the complex interaction between the molten alloy and

nanoparticles by using the ANSYS Fluent Dense Discrete Phase Model (DDPM) and κ - ω turbulence model. The CFD model is described in detail in [21, 22]. To be able to model the nanodispersion over long time periods, the DDPM model is currently uncoupled from the cavitation model.

3 RESULTS AND DISCUSSION

3.1 Modeling Analysis

The predictions of the cavitation and flow are presented in Figure 3 for an A356 liquid alloy at time $t = 2.0 \times 10^{-4}$ s, which is after the onset of cavitation. The onset of cavitation for this alloy system is around 8.8×10^{-6} s [23, 24]. The predicted ultrasonic cavitation region is presented in Figure 3a, where the cavitation phase is hydrogen [21]. The cavitation region is relatively small at time $t = 2 \times 10^{-4}$ s, the acoustic streaming is relatively strong, especially in the ultrasonic probe region (see velocity vectors in Figure 3b) and thus the newly created phase can be transported into the bulk liquid quickly. Note that the legend in Fig. 3a shows the volume cavitation region. Figure 4 shows the distribution of the nanoparticles after 30 s. As it can be seen from Figure 4 the streams of nanoparticles are reasonably well dispersed in the matrix. Some agglomeration of nanoparticles can be observed. This is in line with the experimental observations done via SEM and EDS analyses [25].

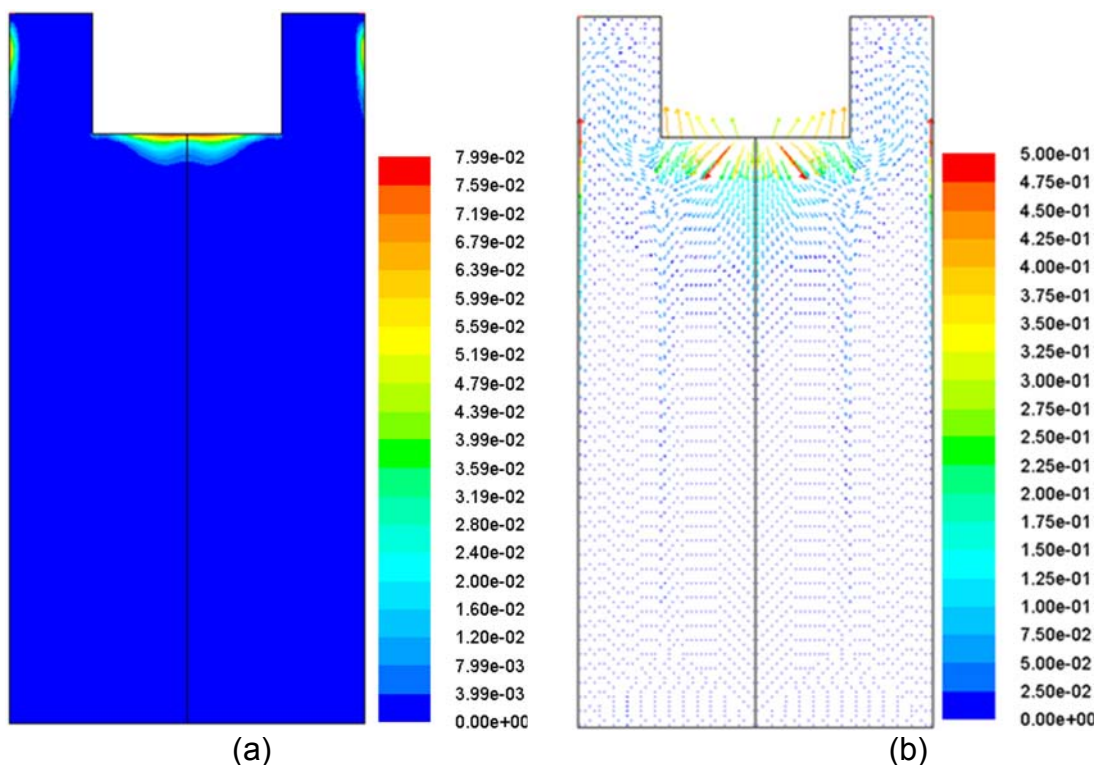


Figure 3. Predicted (a) cavitation region (volume fraction) and (b) velocity vectors (m/s) at $t = 2 \times 10^{-4}$ s.

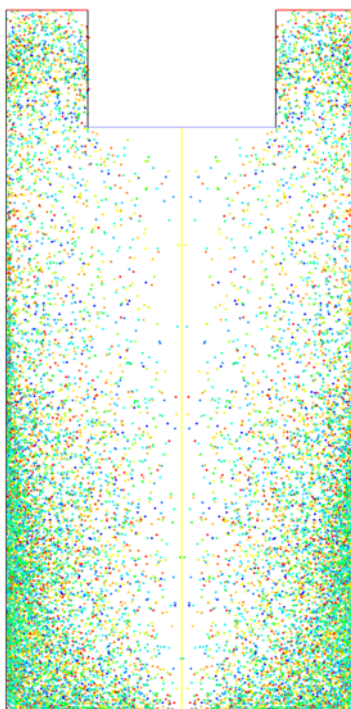


Figure 4. Predicted distribution of the stream of nanoparticles at $t = 30s$.

3.2 Experimental Analysis

Table 2 shows the tensile test results for the as cast 6061 alloy and nanocomposites under different melt treatment conditions. By using the UST treatment and the addition of nanoparticles, the tensile strength almost remains the same. On the other hand, the elongation increases by 45% after the UST treatment and by about 3 times after the UST treatment and the addition of nanoparticles.

Table 2. Tensile testing results for the as-cast 6061 samples

6061 Samples	Tensile strength MPa	Elongation %
Ar Degassed	163.3 ± 9.2	4.7 ± 0.9
UST	154.6 ± 11.3	6.8 ± 1.3
UST+1% SiC	158.6 ± 10.6	13.1 ± 2.4
UST+1% Al ₂ O ₃	163.5 ± 12.9	13.2 ± 1.9

Both the Hall-Petch (grain boundary) and the Orowan (dislocation loop) strengthening mechanisms contributed to the increase of tensile strength. But the agglomeration of nanoparticles and microporosity can decrease the tensile strength of nanocomposite samples. The combination of these effects may be the reason that the tensile strength almost remains the same for 6061 samples. The increase in the elongation of the 6061 samples may be attributed to the slip mode transition produced by the presence of nanoparticles which depends on the matrix/nanoparticles interaction [6, 25].

Table 3 shows the tensile test results for A356 alloy and nanocomposites under different treatment conditions. By using the UST treatment and the addition of nanoparticles, the elongation remains the same while the tensile strength increases after the UST treatment and addition of nanoparticles.

Table 3. Tensile testing results for the as-cast A356 samples

A356 Samples	Tensile strength MPa	Elongation %
Ar Degassed	151.3 ± 6.2	3.4 ± 0.2
UST	172.6 ± 7.9	4.1 ± 0.6
UST+1% SiC	172.0 ± 5.9	4.4 ± 0.5
UST+1% Al ₂ O ₃	177.6 ± 8.2	4.4 ± 0.7

The differences in tensile properties between the as-cast A356 and 6061 samples may be explained from the differences in the Si content in the two types of alloys. A356 alloy has about 7% of Si element while 6061 alloy has only about 0.4-0.8% Si element. The reinforcement-matrix interfaces play an important role in determining the mechanical properties of the nanocomposites. SEM observation of polished and etched A356-1.0%SiC samples revealed that SiC particles appeared to act as substrates for nucleation of Si phase [26]. In A356, SiC and Al₂O₃ nanoparticles may both act as substrate for nucleation of Si phase, which will promote the reinforcement-matrix interface coherency. Thus, the strengthening effects of both UST and nanoparticles will dominate over the weakening effects of nanoparticle agglomeration and microporosity in A356-based nanocomposite.

4 CONCLUSIONS

It is shown in this paper that the CFD model that can simulate the complex phenomena during ultrasonic processing of nano-composites including cavitation and nanodispersion phenomena. The CFD model showed that (i) the cavitation region is relatively small beneath the ultrasonic probe and transferred quickly into the bulk via acoustic streaming and (ii) the nanoparticles are well dispersed in the molten alloy and, assuming that they will not be significantly agglomerated during the solidification process, a finely dispersed nanoparticle composite can be obtained. This is in line with the experimental observations done via SEM and EDS analyses.

A comparison between mechanical properties of 6061 and 356 alloys and nanocomposites was shown in this study. It was found that a significant improvement in the ductility of the as-cast 6061 nanocomposite was achieved after the addition of the Al₂O₃/SiC ceramic nanoparticles via ultrasonic processing while no increase in tensile strength was observed. Cross slip in non-basal slip planes activated by the presence of nanoparticles could be the mechanism of the ductility improvement. This is opposite to the as-cast A356 nanocomposite where it was observed that the tensile strength increased but the ductility remained almost constant. The differences in tensile properties between the as-cast A356 and 6061 samples may be explained from the differences in the Si content in the two types of alloys.

REFERENCES

- 1 Su B, Yan HG, Chen G, Shi JL, Chen JH, Zeng PL. Study on the preparation of the SiCp/Al-20Si-3Cu functionally graded material using spray deposition. *Materials Science and Engineering: A*. 2010; 527: 6660-6665.
- 2 Seyed Reihani SM. Processing of squeeze cast Al6061-30vol% SiC composites and their characterization. *Mater Design*. 2006; 27: 216-222.

- 3 Bozic D, Dimcic B, Dimcic O, Stasic J, Rajkovic V. Influence of SiC particles distribution on mechanical properties and fracture of DRA alloys. *Materials Design*. 2010; 31: 134-141.
- 4 De Cicco MP, Li X, Turng LS. Semi-solid casting (SSC) of zinc alloy nanocomposites. *Journal of Materials Processing Technology*. 2009; 209: 5881-5885.
- 5 Goh CS, Wei J, Lee LC, Gupta M. Simultaneous enhancement in strength and ductility by reinforcing magnesium with carbon nanotubes. *Materials Science and Engineering: A*. 2006; 423: 153-156.
- 6 Elshalakany AB, Osman TA, Khattab A, Azzam B, Zaki M. Microstructure and Mechanical Properties of MWCNTs Reinforced A356 Aluminum Alloys Cast Nanocomposites Fabricated by Using a Combination of Rheocasting and Squeeze Casting Techniques. *Journal of Nanomaterials*. 2014; 2014: 14.
- 7 Mussert MK, Vellinga WP, Bakker A, Van Der Zwaag S. A nano-indentation study on the mechanical behaviour of the matrix material in an AA6061 - Al₂O₃ MMC. *Journal of Materials Science*. 2002; 37: 789-794.
- 8 Akio K, Atsushi O, Toshiro K, Hiroyuki T. Fabrication Process of Metal Matrix Composite with Nano-size SiC Particle Produced by Vortex Method. *J. Jpn. Inst. Light Met.* 1999; 49: 149-154.
- 9 Chen XF, Baburai EG, Froes FH, Vassel A. Ti-6Al-4V/SiC Composites by Mechanical Alloying and Hot Isostatic Pressing. *Proc. Adv. Part. Mater. Processes*. 1997; 185-192.
- 10 Urtiga Filho SL, Rodriguez R, Earthman JC, Lavernia EJ. Synthesis of Diamond Reinforced Al-Mg Nanocrystalline Composite Powder Using Ball Milling. *Mater. Sci. Forum*. 2003; 416-418: 213-218.
- 11 Groza JR. Sintering of nanocrystalline powders. *Int. J. Powder Metall.* 1999; 35: 59-66.
- 12 Jian X, Xu H, Meek TT, Han Q. Effect of power ultrasound on solidification of aluminum A356 alloy. *Materials Letters*. 2005; 59: 190-193.
- 13 Khalifa W, Tsunekawa Y, Okumiya M. Effect of ultrasonic melt treatment on microstructure of A356 aluminium cast alloys. *Int. J. Cast. Metals Res.* 2008; 21: 129-134.
- 14 Eskin GI. Effect of ultrasonic (cavitation) treatment of the melt on the microstructure evolution during solidification of aluminum alloy ingots. *Zeitschrift für Metallkunde*. 2002; 93: 502-507.
- 15 Xu H, Jian X, Meek TT, Han Q. Degassing of Molten Aluminum A356 Alloy Using Ultrasonic Vibration. *Materials Letters*. 2004; 58: 3669-3673.
- 16 Meek TT, Jian X, Xu H, Han Q. Ultrasonic processing of materials. US Department of Energy, Washington DC, USA, 2006.
- 17 Hielscher T. Ultrasonic production of nano-size dispersions and emulsions. Dans *European Nano Systems Workshop - ENS 2005*, Paris, France, 2005.
- 18 Lan J, Yang Y, Li X. Microstructure and microhardness of SiC nanoparticles reinforced magnesium composites fabricated by ultrasonic method. *Materials Science and Engineering: A*. 2004; 386: 284-290.
- 19 Cao G, Choi H, Konishi H, Kou S, Lakes R, Li X. Mg-6Zn/1.5%SiC nanocomposites fabricated by ultrasonic cavitation-based solidification processing. *Journal of Materials Science*. 2008; 43: 5521-5526.
- 20 Yan J, Xu Z, Shi L, Ma X, Yang S. Ultrasonic assisted fabrication of particle reinforced bonds joining aluminum metal matrix composites. *Mater Design*. 2011; 32: 343-347.
- 21 Nastac L. Numerical Modeling of Fluid Flow and Solidification Characteristics of Ultrasonically Processed A356 Alloys. *ISIJ International*. 2014; 54: 1830-1835.
- 22 Zhang D, Nastac L. Numerical modeling of the dispersion of ceramic nanoparticles during ultrasonic processing of aluminum-based nanocomposites. *Journal of Materials Research and Technology*. 2014; 3: 296-302.
- 23 Nastac L. Mathematical Modeling of the Solidification Structure Evolution in the Presence of Ultrasonic Stirring. *Metallurgical and Materials Transactions B*. 2011; 24: 1297-1305.

- 24 Nastac L. Multiscale modeling of the solidification microstructure evolution in the presence of ultrasonic stirring. IOP Conference Series: Mater. Science. Eng [internet]. 2012; 33: 012079. Available at: <http://iopscience.iop.org/1757-899X/33/1/012079>.
- 25 Jia S, Zhang D, Nastac L. Experimental and Numerical Analysis of the 6061-Based Nanocomposites Fabricated via Ultrasonic Processing. Journal of Materials Engineering and Performance [internet]. 2015; Available at: <http://link.springer.com/article/10.1007/s11665-015-1467-4>.
- 26 Zhou W, Xu ZM. Casting of SiC reinforced metal matrix composites. Journal of Materials Processing Technology. 1997; 63: 358-363.